North American Academic Research

TWASP

Research

Analysis of Os-Cfar and Ml-Cfar for a detection of a target in a noisy environment

Abdel Hamid Mbouombouo Mboungam[1]*, Zhi Yongfeng[1], Merlin Thibaut Mouadje Kuate[2]

[1]School of Automation, Northwestern Polytechnical University, CHINA

[2]School of Energy and Electrical Engineering, Chang'an University, CHINA

Abstract: The purpose of this work is to address the problem of detection in an inhomogeneous environment with clutter distributed in a homogeneous way for two types of detectors the OS and the ML-CFAR. The clutter is assumed to be a sea clutter represented by a Weibull distribution. In order to determine which detector is the best, a comparison was made for several parameters by simulation related to the variation of the signal-to-clutter ratio (*SCR*) and some cells N and the probability of false alarm also for different values of the shape parameter c is known or unknown. The results show that the ML-CFAR detector improved performance over the OS-CFAR detector.

Keywards: CFAR detector, clutter, target model, Radar, SCR.

*Corresponding Author

Accepted: 06 January, 2023; **Published**: 15 January, 2023

How to cite this article*: Abdel Hamid Mbouombouo Mboungam, Zhi Yongfeng, Merlin Thibaut Mouadje Kuate (2023). Analysis of Os-Cfar and Ml-Cfar for a detection of a target in a noisy environment. North American Academic Research, 6(1), 1-29. doi: https://doi.org/10.5281/zenodo.7537557*

Conflicts of Interest: There are no conflicts to declare.

Publisher's Note: NAAR stays neutral about jurisdictional claims in published maps/image and institutional affiliations.

Introduction

Nowadays, radar has become an essential instrument for maritime navigation and Aerial safety. Radar signal detection is a complex task that requires special equipment and considerable signal processing computation. For a given detection system, not all detectable objects do not have the same importance, and an object worthy of interest for a system considered without interest and even inconvenient for another (weather radar designed to detect precipitation, which constitutes a hindrance for the detection of aircraft by an air surveillance radar).

In radar systems, the signal from the target is separated from the unnecessary clutter which comes from the reflection of unwanted objects such as the ground, trees, the sea, etc. To eliminate these disturbances, conventional detection based on a fixed threshold causes a considerable increase in the probability of false alarm (deciding that an object is present when it is absent). Adaptive methods choose to analyze and improve radar detection. Devices using these methods are called CFAR detectors. The Monte Carlo simulation results justify the advantage they brought.

In this work, we propose to deal with the problem of detection in an environment not homogeneous with clutter distributed in a homogeneous way for two types of detectors, the OS-CFAR and ML-CFAR. The clutter is assumed to

be a sea clutter represented by a Weibull distribution, and the shape parameter will be assumed to be either known or unknown. We also compare the OS-CFAR and the WH-CFAR (Weber-Haykin) estimator. Also, a comparison is made for the ML-CFAR detector in both cases of known C and estimated C. Finally, a comparison between the OS-CFAR and ML-CFAR detectors is made.

Our work is organized as follows, in the first part a brief reminder on the generalities of CFAR detection is presented. In the second part, we analyze the OS and ML-CFAR detectors in a Weibull distribution clutter. We then present in the third part the results obtained by MATLAB programming using the Monte Carlo method. We interpret the different graphs obtained according to the variation of the *SCR*. Finally a conclusion is presented.

1. Generalities on CFAR detection

1.1. Detection theory

Detection is the operation that consists in deciding on the existence or not of targets in the search space. The basic principle of target detection is to compare the signal received at a decision threshold [1].

A test of binary hypotheses formalizes this problem. The first null hypothesis H_0 represents a zero (absence) where the received signal consists of noise only, and hypothesis H_1 represents a one (presence) where the received signal comes from the echoes of the target added to the noise.

The above situation can be described by a source emitting two outputs at various times. The outputs are designated as hypotheses; the null hypothesis H_0 represents a zero (no target) where the received signal is received and is noise only from noise echoes.

$$\begin{cases} H_0: y(t)=n(t) \\ H_1: y(t)=n(t)+s(t) \end{cases}$$

Hypotheses are based on observations represented by random variables. Based on the observed values of these random variables, the set of values that the random variable X takes constitutes the observation space Z. This space observation is divided into two regions Z_0 and Z_1, such that if X is in Z_0, then the receiver decides in favor of H_0. In contrast, if X is in Z_1, the receiver decides in favor of H_1, following the indications of the figure below. The Union of Z_0 and Z_1 corresponds to the observation space Z, i.e.,

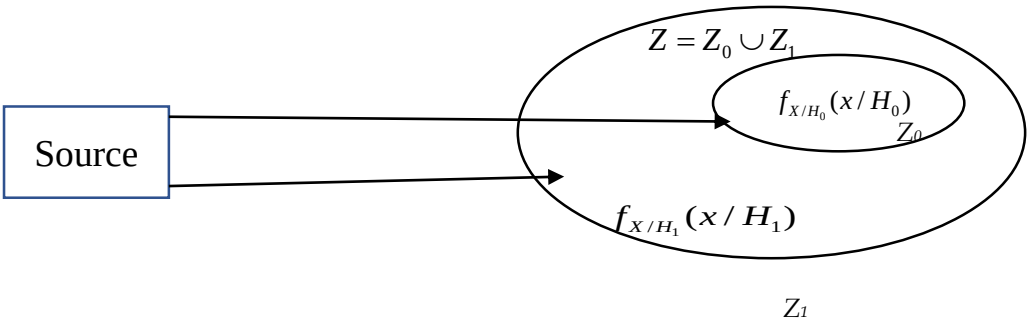

Figure 1: Region of decision

Where X represents the observers (scalars, vectors, or samples of a signal taken over a time interval). The probability density functions corresponding to each hypothesis are:

$$f_{X/H_1}(x/H_1) \qquad f_{X/H_0}(x/H_0)$$

Whenever a decision is made based on certain criteria, for this binary hypothesis testing problem, we have four cases that can occur:

- Decide H_0 and H_0 true ($H_0=1$ and $D_0=1$)
- Decide H_0 and H_1 true ($H_1=1$ and $D_0=1$)
- Decide H_1 and H_0 true ($H_0=1$ and $D_1=1$)
- Decide H_1 and H_1 true ($H_1=1$ and $D_1=1$)

These four possibilities are associated with four probabilities which will be used to judge the performance of a decision criterion.

- $P(D_0 / H_0)$ corresponds to a situation with no alarm.
- $P(D_1 / H_0) = 1- P(D_0 / H_0)$ corresponds to a false alarm probability.
- $P(D_0 / H_1)$ corresponds to a probability of non-detection P_m.
- $P(D_1 / H_1) = 1- P(D_0 / H_1) = 1- P_m$ correspond to the probability of the target detection.

We have:

$$P(D_i / H_i) = \int_{Z_i} f_{X/H_j}(x / H_j)dx \quad (1)$$

To eliminate the Z_i regions, it will be necessary to define an optimal detection strategy that will maximize the probability of detection P_d while guaranteeing a low probability of false alarm P_{fa}.

$$P(D_i / H_i) = \int_{Z_i} f_{X/H_j}(x / H_j)dx \quad (2)$$

1.1.1. Decision criterion

To determine the partition (D_0, D_1) of Z it is necessary to have a criterion that will make it possible to compare the various manners of doing it. Several criteria are used here, which differ according to the information available concerning the cost of the decisions and the probabilities of the hypotheses [2]:

- Bayes criterion (at minimum average cost)
- Neyman-Pearson criterion

1.2. Bayes criterion

This method requires prior knowledge of a set of data:

- The probabilities of appearance of the two hypotheses H_0 and H_1. These probabilities of hypotheses H_0 and H_1 which are denoted $P(H_0)$ and $P(H_1)$ or more simply P_0 and P_1 respectively, with the condition:

$$P_0 + P_1 = 1$$

- The detection costs C_{ij} are assigned to the couples $(D_i H_i)$ with the condition:

$$C_{ii} < C_{ij} \qquad \forall i \neq j$$

The purpose of the Bayes criterion is to determine the decision rule that leads to a minimum average cost. The Bayes cost function, also called the risk function, *R=E(C)*, is given by:

$$R = E(C) = \sum_{j=0}^{1}\sum_{i=0}^{1} C_{ij} P(D_i, H_j) \tag{3}$$

From Bayes' rule:

$$P(D_i, H_j) = P(D_i, H_j) * P(H_i) \tag{4}$$

$$R = P_0 C_{00} P(D_0 / H_0) + P_1 C_{01} P(D_0 / H_1) + P_0 C_{10} P(D_1 / H_0) + P_1 C_{11} P(D_1 / H_1) \tag{5}$$

The conditional probabilities $P(D_i/H_j)$; $i,j=0,1$ depending on the observation regions are:

$$P\left(D_i / H_j\right) = P\left\{Decide\ D_i / H_j is\ true\right\} = \int_{Zi} f_{X/H_1}(x / H_j)dx \tag{6}$$

$$R = P_0 C_{10} + P_1 C_{11} + \int_{Z0} \{P_1(C_{01} - C_{11}) f_{X/H_1}(x / H_j) - P_0(C_{10} - C_{00}) f(x / H_0)\}dx \tag{7}$$

We observe that the quantity $P_0C_{10}+P_1C_{11}$ is constant, regardless of how we assign the points in the observation space.

As a result, the risk is minimized by choosing the decision region Z_0 to include only the points of *Y*, for which the second limit is larger [3].

$$\Lambda(X) = \frac{f_{X/H_1}(x / H_1)}{f_{X/H_0}(x / H_0)} \underset{<H_0}{\overset{>H_1}{}} \frac{P_0(C_{10} - C_{00})}{P_1(C_{01} - C_{11})} \tag{8}$$

Where: $\Lambda(X)$ is the likelihood ratio and $\eta = \frac{P_0(C_{10} - C_{00})}{P_1(C_{01} - C_{11})}$ decision threshold.

In general, the costs and the probability of radar detection are worth the:

$$C_{ij} = 0, C_{ij} = 1, P_0 = P_1 = \frac{1}{2}$$

The problem with this criterion is that it requires knowledge of the probabilities of $P(H_1)$ and $P(H_0)$ and the costs C_{ij}, in general, when this is not the case, other criteria are used, such as NEYMAN PEARSON.

1.3. Neyman-Pearson criterion

Unlike the Bayes criterion, the Neyman-Pearson criterion does not require many assumptions; it corresponds to real situations. This criterion proposes to set the probability of false alarm *Pfa* at a level α. This value is established by a specification from which an objective function *J* is built [4]:

$$J(\lambda) = P_m + \lambda(Pfa - \alpha) \tag{9}$$

Where: $\lambda(\lambda \geq 0)$ is the Lagrange multiplier. We note that for an observation space Z given, there are several decision regions Z_1 for which $Pfa=\alpha$.

The Lagrange multiplier is defined as maximizing the probability of detection or minimizing the probability of P_m.

$$J(\lambda) = \int_{Z_1} f_{X/H_1}(x/H_1)dx + \lambda\left[\int_{Z_1} f_{X/H_0}(x/H_0)dx - \alpha\right] \tag{10}$$

Since $Z = Z_0 \cup Z_1$

So, equation (5) becomes:

$$J(\lambda) = \lambda(1-a) + \int_{Z_0}\left[f_{X/H_1}(x/H_1) - \lambda f_{X/H_0}(x/H_0)\right]dx \tag{11}$$

J is minimized when the values for which $f_{X/H_1}(x/H_1) > f_{X/H_0}(x/H_0)$ are assigned to the decision region Z_1 [3].

The solution to the inequality is:

$$\frac{f_{X/H_1}(x/H_1)}{f_{X/H_0}(x/H_0)} < \lambda \tag{12}$$

Moreover, we can give the decision rule:

$$\Lambda(X) = \frac{f_{X/H_1}(x/H_1)}{f_{X/H_0}(x/H_0)} \underset{<_{H_0}}{>^{H_1}} \lambda \tag{13}$$

$f_{X/H_0}(x/H_0)$ Represent the conditional probability of X under the hypothesis H_0; where λ is chosen in such a way as to satisfy the constraint [4].

$$Pfa = \int_{\lambda}^{\infty} f_{X_0/H_0}(x/H_0)dx = \alpha \tag{14}$$

The Neyman-Pearson criterion is applied in several fields because it does not require knowledge of the probabilities of the hypotheses H_1 and H_0 as well as the cost C_{ij}, but its drawback is that it can only be used when the process is stationary, which is not always the case in practice. It caused the birth of adaptive sensing.

1.3.1. CFAR detector

The false alarm probability is very sensitive to changes in the noise power variation; for this reason, the use of a fixed threshold in conventional detection is not applicable. Figure 2 shows an increase in the false alarm probability by a factor of 10^{-4} caused by a slight increase in noise power of the order of 3 dB. [2]

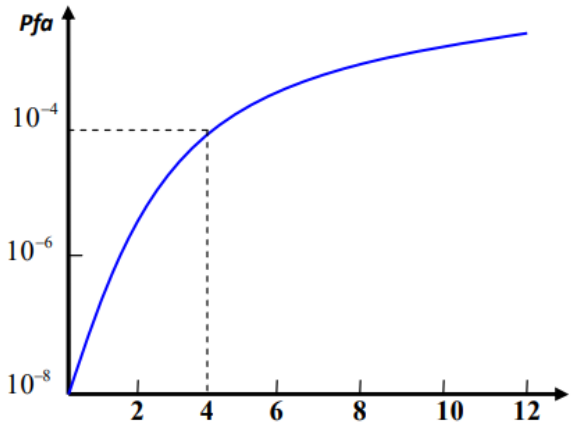

Figure 2: Effect of increasing noise power on false alarm probability

The CFAR is a model placed in the signal processing part of the radar receiver; after reception and demodulation of the radar echoes, these travel through a series of cells of odd numbers.

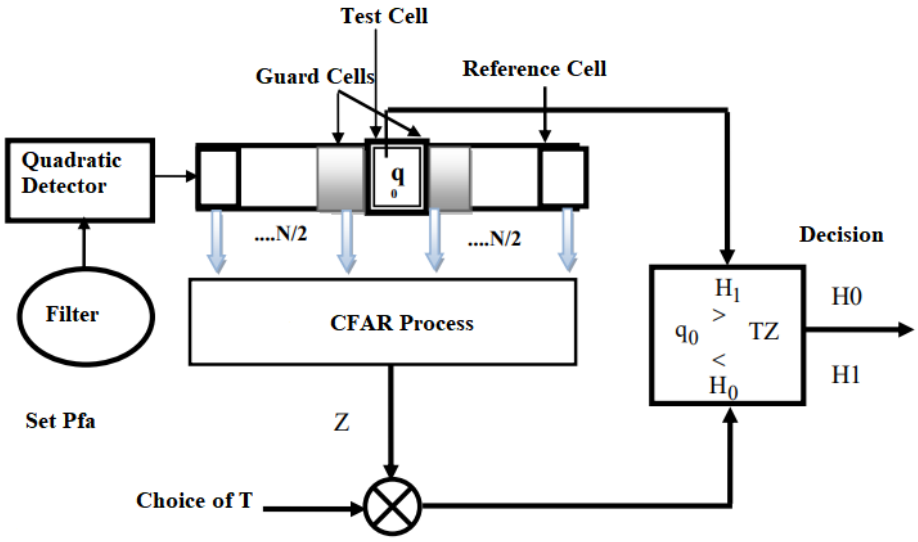

Figure 3: Diagram of a CFAR [2]

The "cell under test" is the central cell; it contains the signal to be detected. As part of the estimation of the power of clutter, two windows grouping "reference" cells are placed on either side of the test cell; the window on the right is denoted by the letter U, and the window on the left by the letter V. To prevent overflow of the signal from the cell under test, "guard cells" are neighboring cells that are not included in the estimation procedure [2].

2. Analysis of OS-CFAR and ML-CFAR detectors

In automatic radar detection, the fundamental problem is noise and clutter in the environment in which this detection is made. In addition, the statistical parameters related to noise are generally unknown.

This work's objective is to study the case of sea clutter, where the samples (cells) are distributed according to a Weibull distribution.

2.1. Weibull distribution

The Weibull probability density function is the most suitable function to represent the sea and land clutter at a low shaving angle or in high-resolution situations. The Weibull probability density function is a two-parameter distribution for which the Rayleigh distribution is a particular case. Our study deals with this situation and assumes that a Weibull probability density function can describe the environment.

$$p(x)=\frac{C}{B}\left(\frac{x}{B}\right)^{C-1}\exp\left[-\left(\frac{x}{B}\right)^{C}\right],x\geq 0;C\geq 0;B\geq 0 \tag{15}$$

Where: x (The random variable), B (The scale parameter), C (The form parameter)

2.2. OS-CFAR detector analysis

This detector is based on ordered statistics, classifying the samples in order increasing, and the K^{th} sample is chosen to estimate the noise level. The rank K is generally chosen to be equal to $3N/4$ or $7N/8$ (greater than $N/2$), such that N is the number of reference cells ordered according to the output level.

$$X_{1}\leq X_{2}\leq .....\leq X_{N} \tag{16}$$

Since the quadratic detector depends on X^2, for this, we consider that the parameter Weibull scale B is equal to 1; So:

$$z=\left(\frac{X}{B}\right)^{2}=X^{2} \tag{17}$$

And the probability function:

$$P(z)=\frac{C}{2}\times z^{\frac{C}{2}-1}\times\exp\left(-z^{\frac{C}{2}}\right) \tag{18}$$

The threshold T_z is given by:

$$T_{z}=\alpha\times z_{k} \tag{19}$$

For samples of amplitude X_i are independent identically distributed (IID) with a Rayleigh probability density function, Rohling showed that the relationship between a false alarm and the scale factor is given by [5]:

$$Pfa=\frac{N!(\alpha+N-K)!}{(N-K)!(\alpha+N)!} \tag{20}$$

Assuming amplitude samples for a medium described by (IID), X is the random variable with a Weibull PDF given by the equation (18). Then choosing the parameter of form C=2, the Weibull probability density function reduces to a probability density function Rayleigh.

The following figure shows the Pfa represented as a function of C when the scale factor has been set for a $Pfa=10^{-5}$.

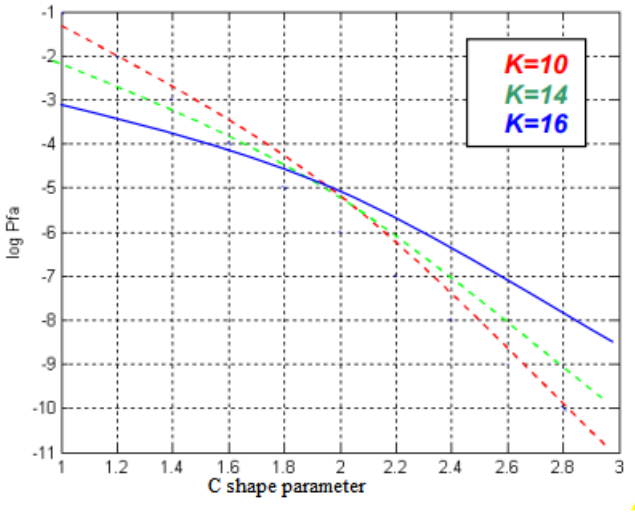

Figure 4: Shape parameter as a function of log *Pfa*. (Minimum value $Pfa=10^{-5}$ and C=2)

We can use Rohling's analysis by making an additional substitution and defining the variable random y:

$$y = z^{C/2} \tag{21}$$

The exponential PDF for which Rohling ran his analysis is:

$$P(y) = exp(-y) \tag{22}$$

The threshold for y:

$$T_{y} = \alpha \times y_k \tag{23}$$

Where:

$$T_z = T_y^{2/C} \tag{24}$$

The probability of false alarm is then defined by:

$$Pfa = \int_0^{\infty} \left[\int_{\alpha.Z(K)}^{\infty} -\left[\exp\left(-z^{C/2}\right)\right] dz \right] p\left(z_{(K)}\right) dz_{(K)} \tag{25}$$

After calculating the integral, the probability of false alarm is given by:

$$Pfa = \frac{N!}{(N-K)!} \frac{\left(\alpha^{C/2} + N - K\right)!}{\left(\alpha^{C/2} + N\right)!} \tag{26}$$

This relationship is obtained in the same way as the probability of detection by setting *S=0*, where *S* or *SCR* is the signal-to-clutter ratio.

$$Pd = \frac{N!}{(N-K)!} \times \frac{\left(\frac{\alpha^{C/2}}{1+S} + N - K\right)!}{\left(\frac{\alpha^{C/2}}{1+S} + N\right)!} \tag{27}$$

We can write the two previous equations as follows:

The probability of detection:

$$Pd = \prod_{i=0}^{K-1} \frac{N-i}{N-i+\frac{\alpha^{C/2}}{1+S}} \tag{28}$$

The false alarm probability:

$$Pfa = \prod_{i=0}^{K-1} \frac{N-i}{N-i+\alpha^{C/2}} \tag{29}$$

It will allow us to study the sensitivity of the original OS-CFAR algorithm to changes in the shape parameter.

2.2.1. The first case (known C)

Here the detection threshold is given by:

$$T_z = T \times z_{(K)} \tag{30}$$

Where: $T = \alpha^{2/C}$

Moreover, α represents the multiplication factor for a Rayleigh distribution.

2.2.2. The second case (unknown C)

All the previous equations are applied when the shape parameter C is known. However, when the shape parameter is unknown, the analysis will be changed entirely. For this, we will fix an estimator of $C\hat{C}$ to calculate the probability of detection. The estimator used is that of "Dubey" [5]. This estimator proposes two ordered samples, X_i and X_j, such as:

$$\hat{C} = \frac{\ln\left[-\ln\left(1-h_j\right)\right] - \ln\left[-\ln\left(1-h_i\right)\right]}{\ln X_j - \ln X_i} \tag{31}$$

Where: $h_i = \frac{i}{N+i}$ and $h_j = \frac{j}{N+1}$

We replace $C\ \hat{C}$ in equation (18) with *K=i.* Then the detection threshold will be given by:

$$Z_T = z_i \left(\frac{z_j}{z_i} \right)^{\beta} = z_i^{1-\beta} . z_j^{\beta} \tag{32}$$

Where:

$$\beta \frac{\ln \alpha_i}{\ln\left[-\ln\left(1-h_j\right)\right] - \ln\left[-\ln\left(1-h_i\right)\right]} \tag{33}$$

2.3. ML-CFAR detector analysis

For the CFAR detectors in a Weibull clutter suggested earlier, the adaptive threshold was effectively based on estimating the scale and shape parameters using either moments or order statistics. Both techniques expose the extent of CFAR loss. Additionally, it has been shown that the loss is related to the variance of the estimated parameters. To reduce the variance and the CFAR loss, a CFAR algorithm in which the parameters are estimated using the maximum likelihood (Maximum Likelihood).

The ML-CFAR algorithm is more computationally expensive than the other approach; However, modern processors may be able to handle additional processing, even if it is not implemented, except the performance of the ML algorithm may serve as a comparative benchmark for simpler algorithms.

Subsequently, we will develop the ML-CFAR algorithm and analyze its performance, starting with the simple case in which the shape parameter is known, and moving on to cases in which the two parameters are unknown. For the general case, we show that the ML-CFAR threshold can be effective, as shown in the following figure:

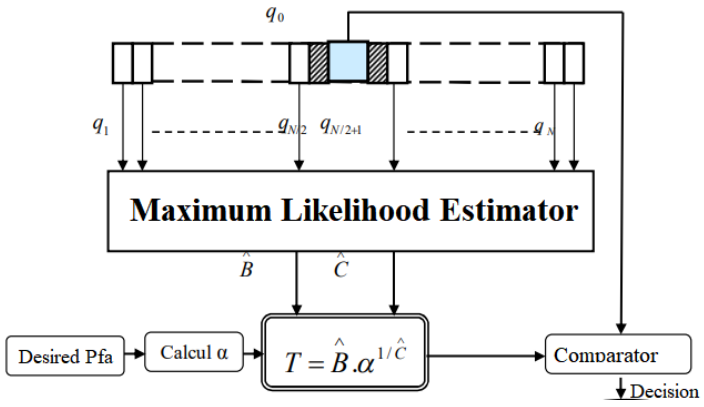

Figure 5: ML-CFAR Detector

By taking the adaptive threshold according to the formula:

$$T = \hat{B}.\alpha^{1/\hat{C}} \tag{34}$$

In the case of *ML*, *B* and *C* are estimated from the *N* samples:

$$x = (x_1, x_2 \ldots\ldots\ldots x_N) \tag{35}$$

Iteratively, we can estimate $\hat{C}$ from the equation:

$$\frac{\sum_{j=1}^{N} x_j^{\hat{C}} \ln x_j}{\sum_{j=1}^{N} x_j^{\hat{C}}} - \frac{1}{\hat{C}} = \frac{1}{N}\sum_{j=1}^{N} \ln x_j \tag{36}$$

Th $\hat{C}$ is is then used to obtain $\hat{B}$ according to the equation:

$$\hat{B} = \left(\frac{1}{N}\sum_{j=1}^{N} C_j^{\hat{C}} \right)^{1/\hat{C}} \tag{37}$$

The coefficient D is a function of the number of reference samples N and the desired false alarm probability. D is independent of the parameters B and C. The probability of detection will be developed for the case of a fluctuating target with a Rayleigh PDF for the two types of targets, Swerling1 and Swerling2.

In this case, an attempt to calculate Pd directly using the exact PDF of the CUT results in a triple integral, which is difficult to evaluate numerically; therefore, one seeks an approximation that is easy to calculate.

We note that when the SCR is high, the contribution of the SCR in the CUT is small, and the exact PDF of this contribution is not very important. We will therefore assume that the CUT contains a Rayleigh target and a Rayleigh clutter with the same mean energy as the Weibull clutter in the reference cells. This approximation becomes exact when the reference cells also present a Rayleigh PDF.

2.3.1. ML-CFAR with a known C shape parameter

We start our analysis with the simplest case in which the shape parameter is known, and we then show that *D* can be expressed explicitly relative to *N*, *Pfa*, and *C* known.

The background noise is represented by a set of *N* samples which are statistically independent and identically distributed (IID), $x_1, x_2, \ldots\ldots\ldots\ldots\ldots x_n$, with a density function of known deformed parameter *C* and an unknown scale parameter *B*.

For the case *C=2*, the PDF becomes of Rayleigh form, for which it has been shown that the estimator of the Maximum-likelihood of *B* is:

$$\hat{B} = \left(\frac{1}{N}\sum_{j=1}^{N} x_j^2 \right)^{1/2} \tag{38}$$

With a threshold of the form:

$$T(x) = \alpha.\hat{B} \tag{39}$$

The false alarm probability is then:

$$Pfa = \left(1 + \frac{\alpha^2}{N}\right)^{-N} \tag{40}$$

We will use the same procedure to determine the threshold, with B estimated, when C is known but is not necessarily equal to 2. Reference [6] shows that for such a case, the ML-CFAR estimator is given by:

$$\hat{B} = \left(\frac{1}{N}\sum_{j=1}^{N} x_j^C\right)^{1/C} \tag{41}$$

And a threshold T equals:

$$T(x) = \alpha.\hat{B} = \alpha.\left(\frac{1}{N}\sum_{j=1}^{N} x_j^C\right)^{1/C} \tag{42}$$

A false alarm occurs when the value in the cell under test (CUT) exceeds the threshold, inputting:

$$Pfa = \int_0^\infty P\left[CUT > T(x)\right] f_x(x)dx \tag{43}$$

The first term in the integral is:

$$P(CUT > T) = \int_t^\infty f(x)dx \tag{44}$$

$$P(CUT > T) = \int_t^\infty \frac{Cx^{C-1}}{B^C} \exp\left[-\left(\frac{x}{B}\right)^C\right] dx \tag{45}$$

$$P(CUT > T) = \exp\left[-\left(\frac{T}{B}\right)^C\right] \tag{46}$$

We replace the threshold of equation (42) in equation (46) we obtain, for the first term in the integral:

$$P(CUT > T) = \exp\left[-\frac{\alpha^C}{N}\sum_{j=1}^{N}\left(\frac{x_j}{B}\right)^C\right] \tag{47}$$

The second term in the integral of equation (43) is the Common PDF for *N* cells is:

$$f_x(x) = \prod_{j=1}^{N} \frac{C}{B}\left(\frac{x_j}{B}\right)^{C-1} \exp\left[-\left(\frac{x_j}{B}\right)^C\right] \tag{48}$$

By inserting equations (47) and (48) into equation (43), we get:

$$Pfa = \prod_{j=1}^{N} \int_{0}^{\infty} \frac{C}{B}\left(\frac{x_i}{B}\right)^{C-1} .\exp\left[-\left(1+\frac{\alpha^C}{N}\right)\left(\frac{x_j}{B}\right)^C\right] dx_i \tag{49}$$

By replacing, $y_i = \left(\frac{x_j}{B}\right)^C$ we obtain:

$$Pfa = \prod_{j=1}^{N} \int_{0}^{\infty} \exp\left[-\left(1+\frac{\alpha^C}{N}\right) y_i\right] dy_i \tag{50}$$

Which gives:

$$Pfa = \left(1+\frac{\alpha^C}{N}\right)^{-N} \tag{51}$$

Equation (51) indicates that the algorithm is indeed CFAR since the false alarm probability is independent of *B*. Substitute equation (51) into equation (42) and obtain the threshold in a simple expression.

$$T(x) = \left[\left(Pfa^{-1/N} - 1\right)\sum_{j=1}^{N} x_j^C\right]^{1/C} \tag{52}$$

The previous analysis assumes a linear detector where the random variable x is distributed with a Weibull distribution for a parameter of form *C*. On the other hand, for a quadratic detector, the random variable $y = x^2$ is also Weibull, with a parameter of equal form *C*/2. The threshold will then become [7]:

$$T(y) = \left[\left(Pfa^{-1/N} - 1\right)\sum_{j=1}^{N} y_j^{C/2}\right]^{2/C} \tag{53}$$

When the shape parameter C is known, the threshold is based on the estimate of the scale parameter, as in equation (42). The probability of detection will therefore be:

$$Pd = \int_{0}^{\infty} P(CUT > \alpha B)\, f_{\hat{B}}(B) dB \tag{54}$$

Where $f_{\hat{B}}(B)$ is the PDF of ML, given by:

$$f_B(y) = \left(\frac{N}{B^C}\right)^N \frac{C}{(N-1)!} y^{C.N-1} \exp\left(-\frac{N.y^C}{B^C}\right) \tag{55}$$

The probability of *CUT* above a threshold *T* is given by:

$$P(CUT > T) = \int_0^\infty f_{CUT}(y)dy \tag{56}$$

We will assume a fluctuating target with a Rayleigh PDF and average power B_t^2. The clutter in the *CUT* will be approximated by a Rayleigh PDF with the same average power as that of the Weibull clutter in the reference cells.

The average power of clutter B_c^2 will be linked with the scale parameter *B*:

$$B_C^2 = B^2\Gamma\left(1+\frac{2}{C}\right) \tag{57}$$

Since the target and the clutter in the *CUT* are Rayleigh distributed, the PDF of the *CUT* will also be Rayleigh distributed.

$$f_{CUT}(y) = \frac{y}{B^2\Gamma\left(1+\frac{2}{C}\right)+B_t^2}\exp\left[\frac{-y^2}{B^2\Gamma\left(1+\frac{2}{C}\right)+B_t^2}\right] \tag{58}$$

We define the *SCR* by:

$$SCR = \frac{B_t^2}{B^2\Gamma\left(1+\frac{2}{C}\right)} \tag{59}$$

Substituting equation (58) into equation (56), we get:

$$P\left(CUT > \alpha\hat{B}\right) = \exp\left[\frac{-\left(\alpha\hat{B}\right)^2}{B^2\left(1+SCR\right)\Gamma\left(1+\frac{2}{C}\right)}\right] \tag{60}$$

Also, by substituting equations (55) and (60) into equation (54), we will find Pd:

$$Pd = \int_0^\infty \exp\left[\frac{-(\alpha.y)^2}{B^2(1+SCR)\Gamma\left(1+\frac{2}{C}\right)}\right]\left(\frac{N}{B^C}\right)^N \cdot \frac{C.y^{C.N-1}}{(N-1)!}\exp\left(\frac{-N.y^C}{B^C}\right)dy \tag{61}$$

Substitute: $$z = \frac{N.y^C}{B^C} \tag{62}$$

We obtain the result for the detection probability when *SCR>>1*:

$$Pd = \frac{1}{(N-1)!}\int_0^{\infty} z^{N-1} \exp\left[\frac{-\alpha^2}{(1-SCR)\Gamma\left(1+\frac{2}{C}\right)}\left(\frac{z}{N}\right)^{2/C}\right] dz \tag{63}$$

For the case of Rayleigh clutter (*C*=2), this integral is solved explicitly, reducing it to the known result:

$$Pd = \left(1+\frac{\alpha^2}{N(1+SCR)}\right)^{-N} \tag{64}$$

Equation (63) is an approximate expression because, even though the clutter in the reference cells follows a Weibull distribution, the *CUT* is assumed to follow a distribution Rayleigh (with the same average power). To verify the accuracy of this approximation, we compare the Pd, which uses equation (63), with the Monte-Carlo simulation in which the *CUT* contains a Weibull clutter (and a Rayleigh target). The results are given in Figure 6.

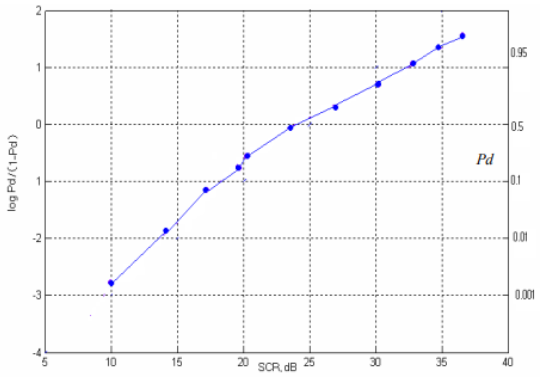

Figure 6: The probability of detection as a function of *SCR*. *Pfa=10*$^{-5}$; *C=1*; *N=16*.

This curve is a theoretical approximation in which the cell under test is assumed to contain a target plus a Rayleigh noise. The dots represent Monte Carlo results in which the *CUT* contains the target plus the correct Weibull distribution noise.

Each point is obtained from 1000 Monte Carlo iterations. For low *SCR*, we look for the actual *Pd* to be somewhat higher than that predicted by equation (63).

2.3.2. ML-CFAR with an unknown *C*-shape parameter

When the scale parameter and the shape parameter are unknown, they need to be estimated simultaneously from the reference cells. The adaptive threshold will be based on the estimated values $\hat{B}$ *and* $\hat{C}$. In this section, we will derive the estimated values $\hat{B}$ *and* $\hat{C}$, which ensure that the threshold described by equation (35) is indeed a CFAR detector; then, we will discuss the relationship between the coefficient α and the false alarm probability *Pfa*.

- **The estimator of *the C* shape parameter and *B* scale parameter:**

To obtain the *ML* estimator, we derive the logarithm of the standard PDF *f(x)* of the *N* reference cells for the parameters *B* and *C*, and then we set the derivative to zero. The resulting equations can be solved repeatedly to obtain the *ML* estimator of *B* and *C*. By assuming the independence between reference cells, the standard PDF is given by:

$$f(x)=\left(\frac{C}{B^C}\right)^N\prod_{j=1}^{N}\left[x_j^{C-1}\exp\left(-\frac{x_j^C}{B^C}\right)\right] \tag{65}$$

For which one we obtain:

$$\ln f(x)=N\ln C-N.C\ln B+(C-1)\sum_{N-1}^{N}\ln x_j-\frac{1}{B^C}\sum_{j=1}^{N}x_j \tag{66}$$

$$\frac{\partial\ln f(x)}{\partial B}=-\frac{NC}{B}+\frac{C}{B}\sum_{j=1}^{N}\left(\frac{x_j}{B}\right)^C \tag{67}$$

$$\frac{\partial\ln f(x)}{\partial C}=\frac{N}{C}-N\ln B+\sum_{j=1}^{N}\ln x_j-\sum_{j=1}^{N}\left(\frac{x_j}{B}\right)^C\ln\left(\frac{x_j}{B}\right) \tag{68}$$

By letting: $\dfrac{\partial\ln f(x)}{\partial B}=0$

We obtain: $$\hat{B}^{\hat{C}}=\frac{1}{N}\sum_{j=1}^{N}\left(\frac{x_j}{B}\right) \tag{69}$$

The same for equation (68), we use equation (69):

$$\frac{\sum_{j=1}^{N}x_j^{\hat{C}}\ln x_j}{\sum_{j=1}^{N}x_j^{\hat{C}}}-\frac{1}{N}\sum_{j=1}^{N}\ln x_j=\frac{1}{\hat{C}} \tag{70}$$

Equation (70) can be solved iteratively to obtain $\hat{C}$, which will then be used in equation (69) to obtain $\hat{B}$.

To justify the choice of the threshold as described by equation (35), we first note that when *B* and *C* are known precisely in equation (46), the false alarm probability is described by:

$$Pfa=\exp\left[-\left(\frac{T}{B}\right)^C\right] \tag{71}$$

Where: $$T=B(-\ln Pfa)^{1/C} \tag{72}$$

On the other hand, when B and C are not precisely known and are replaced by their estimated values which are not without errors, the given threshold exhibits a larger *Pfa*, predicted by equation (71). To compensate for this, we replace (*-ln Pfa*) with a parameter α, which can be checked to determine the desired *Pfa*. The threshold is therefore given by:

$$T = \hat{B}.\alpha^{1/\hat{C}} \tag{73}$$

For many references cells N and a relatively high *Pfa*, α is slightly higher than (*-ln pfa*). A study in reference [6] on the properties of CFAR detectors, to the heuristic approach which led to equation (73); the simulation technique gives results between the factor α and *Pfa* for two values of N (16 cells and 32 cells). These results are plotted in the figure below.

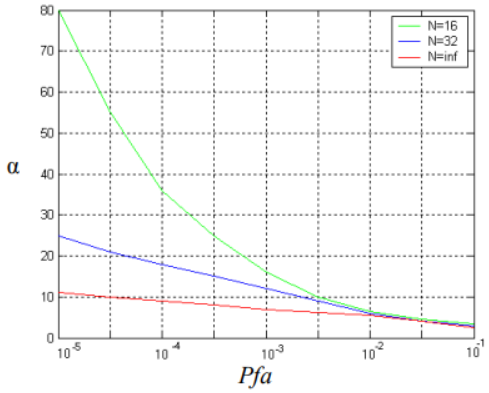

Figure 7: The factor α as a function of Pfa.

We also added the curve of (*-ln Pfa*); for which α converges when N tends to infinity. In Figure 7, each point on the curve corresponding to *N=32* is obtained from 100,000 iterations, and each point on the curve *N=16* is obtained from 50,000 iterations. The curves are obtained using linear interpolation between points without smoothing [7].

In this part, we have defined the Weibull distribution which represents the sea clutter from the probability density function PDF. This PDF has been developed to obtain a function of the false alarm probabilities *Pfa*, the detection probability *Pd* and the detection threshold *T* for the OS-CFAR and ML-CFAR detectors. The function *Pfa* generally corresponds to a *C* form parameter which varies, and this variation makes it possible to carry out the analysis for two cases, the first concerns the case where the *C* form parameter is known and the other, the case where the *C* form parameter is unknown (estimated). The analysis used in this part has made it possible to find the different formulas of the detection threshold to allow the simulation of the detection for the different types of detectors presented above.

3. Simulation and interpretation of results

3.1. Simulation and interpretation of results

In the above, we have analyzed the performance of the detectors OS-CFAR and ML-CFAR. We have dealt with detection problems in an environment where the clutter is a sea clutter with a Weibull distribution and a proposed shape parameter C known a priori and unknown. This part presents applications for this kind of system, several tests have been carried out and the results found are presented here, as well as their interpretation to establish a comparison for each detector in each situation.

Here, we assumed that the valuable signal follows a Weibull law, so the background noise is represented by a set of N samples that are statistically independent and identically distributed (IID) (homogeneous clutter).

3.2. OS-CFAR detector

According to the equation of the probability of false alarm (29), we notice that the latter depends on the number of cells N, of the multiplication factor α, of the shape parameter C, and the sample K:

3.2.1. C shape parameter is known

This section presents the variation of the detection probability Pd for an OS-CFAR detector as a function of the SCR. The false alarm probability equation (28) was programmed from which the following tables were obtained:

Parameter	Cells	Samples	T		
	N	K	$Pfa=10^{-2}$	$Pfa=10^{-4}$	$Pfa=10^{-6}$
C=1	8	6	34.4527	352.5047	2180.6
	12	8	23.6435	173.4714	736.9
	16	12	19.5815	122.7708	439.1
	24	18	16.2038	87.2507	265.5

Table 1: T values for different values of *Pfa*. Case of OS-CFAR (C=1)

Parameter	Cells	Samples	T		
	N	K	$Pfa=10^{-2}$	$Pfa=10^{-4}$	$Pfa=10^{-6}$
C=2	8	6	5.8697	18.7752	46.6973
	12	8	4.8625	13.1709	27.1452
	16	12	4.4251	11.0802	20.9542
	24	18	4.0254	9.3409	16.2933

Table 2: T values for different values of *Pfa*. Case of OS-CFAR (C=2)

Parameter	Cells	Samples	T		
	N	K	$Pfa=10^{-2}$	$Pfa=10^{-4}$	$Pfa=10^{-6}$
C=3	8	6	3.2540	7.0641	12.9677
	12	8	2.8702	5.5772	9.0323
	16	12	2.6954	4.9701	7.6006
	24	18	2.5305	4.4353	6.4270

Table 3: T values for different values of *Pfa*. Case of OS-CFAR (C=3)

Figures 8, 9, and 10 represent the variation of the detection probability Pd as a function of the SCR, the number of cells N, and the shape parameter C for a probability of false alarm equals 10^{-4}.

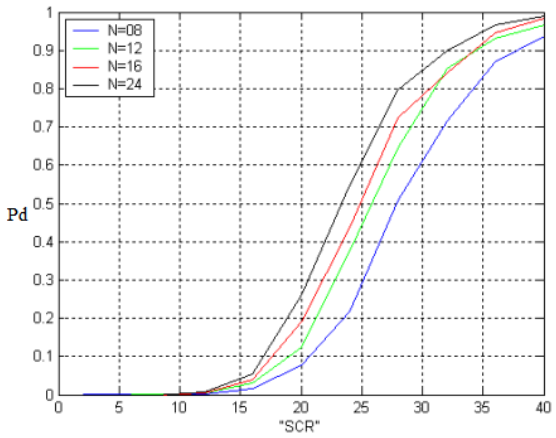

Figure 8: The probability of detection as a function of the *SCR*. Case of the OS-CFAR detector for *C=1* and *Pfa=10*$^{-4}$

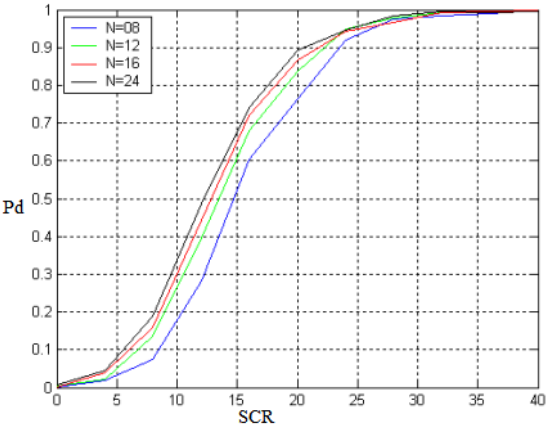

Figure 9: The probability of detection as a function of the *SCR*. Case of the OS-CFAR detector for *C=2* and *Pfa=10*$^{-4}$

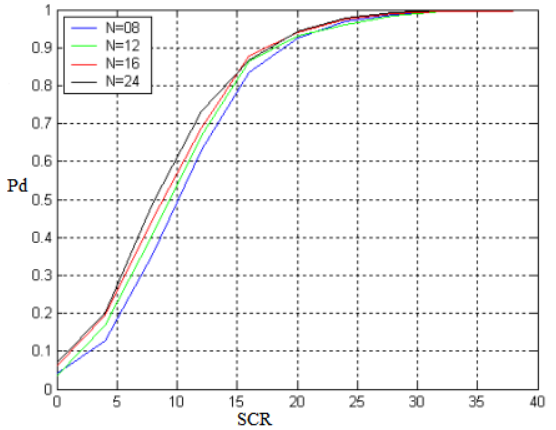

Figure 10: The probability of detection as a function of the *SCR*. Case of the OS-CFAR detector for *C=3* and *Pfa=10*$^{-4}$

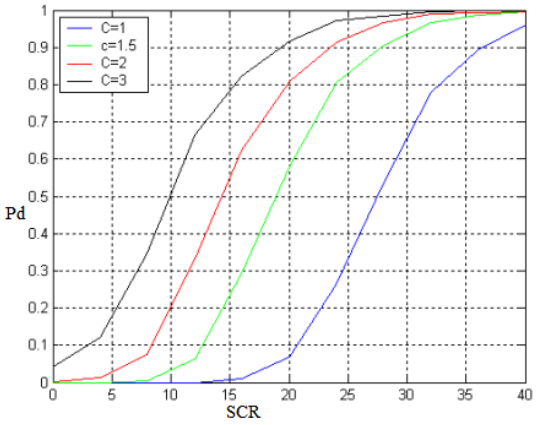

Figure 11: The probability of detection as a function of the *SCR*. Case of the OS-CFAR detector for *N=16* and $Pfa=10^{-5}$

From this figure we can see that the probability of detection Pd improves with the increase of the shape parameter *C*. For a value of *C* equal to 2, the system is more reliable than in another case; the graph, in this case, starts from the origin and grows with increasing *SCR*.

In figure 12, we illustrate the variation of the probability of detection according to the *SCR* by varying the probability of false alarm *Pfa* where the shape parameter *C* is equal to 2, and the number of cells equals 16.

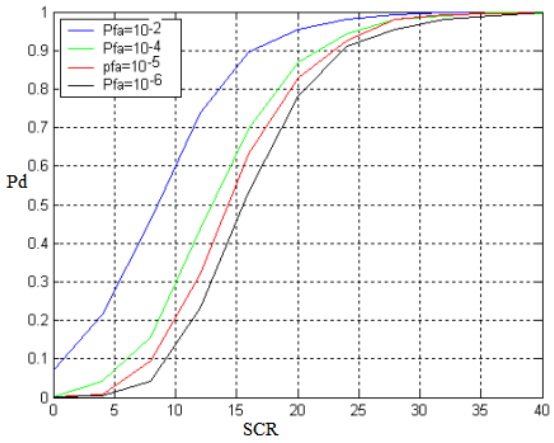

Figure 12: The probability of detection as a function of the *SCR*. Case of the OS-CFAR detector for *N=16* and *C=2*

3.2.2. C shape parameter is unknown

In the part of the analysis, we saw that Weber Haykin showed that when the *C* shape parameter is unknown, the OS-CFAR algorithm can be obtained using two samples of order Z_i and Z_j.

In this work, we set *i* equal to 2, 2, 3, and 4 for *j* equal *N*, which are 8, 12, 16, and 24 respectively. We note that this choice of *i* and *j* causes a minimal CFAR loss. The table below represents the values of factor α, which will be replaced in the estimator of *C*.

Cells	Samples	Samples	α_i		
N	*i*	*j*	$Pfa=10^{-2}$	$Pfa=10^{-4}$	$Pfa=10^{-6}$
8	2	8	67.34	740.8	7476

12	2	12	103.4	1137.4	11478
16	3	16	54.53	307.7	1483
24	4	24	48.58	202.2	688

Table 4: Values of α_i for different values of *Pfa* in the case of OS-CFAR

The curves in Figures 13, 14, and 15 represent the variation in the probability of detection as a function of the *SCR* and the number of cells *N* for a *Pfa* equal to 10^{-4}.

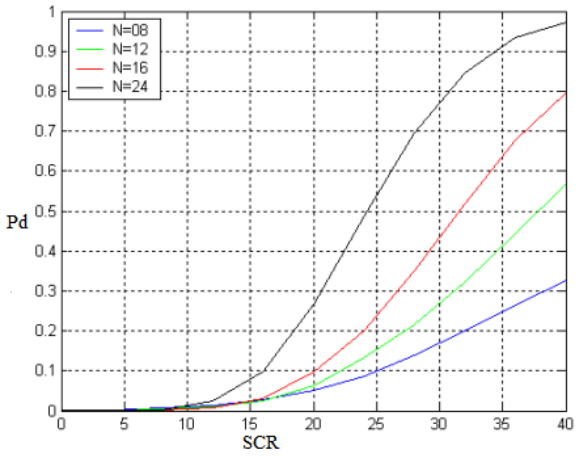

Figure 13: The probability of detection as a function of the *SCR*. Case of the OS-CFAR detector. *C* estimated for *C=1* and *Pfa=10*$^{-4}$

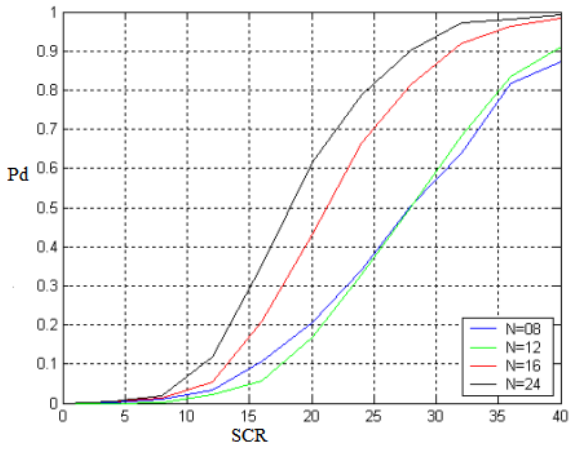

Figure 14: The probability of detection as a function of the *SCR*. Case of the OS-CFAR detector. *C* estimated for *C=2* and *Pfa=10*$^{-4}$

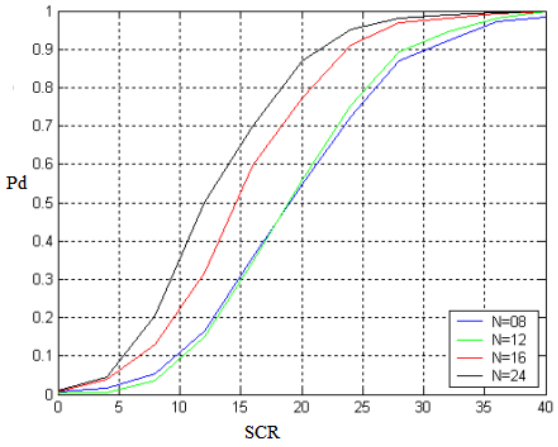

Figure 15: The probability of detection as a function of the *SCR*. Case of the OS-CFAR detector. *C* estimated for *C=3* and $Pfa=10^{-4}$

Figure 16 illustrates the variation of the probability of detection as a function of the *SCR* by varying the *C*-shape parameter.

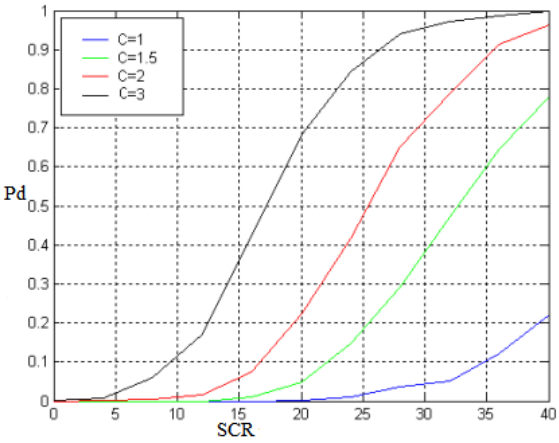

Figure 16: The probability of detection as a function of the *SCR*. Case of the OS-CFAR detector for *N=16* and $Pfa=10^{-5}$

We chose the number of cells *N* equal to 16 and the two samples *i* and *j* of the estimator of "Dubey", such that *i* equals 3 and *j* equals 16 because this estimator presents a minimum loss (CFAR loss) of about 9.4 dB. In this case, the deviation of the estimate of *C* is equal to 0.49, which is represented by a significant difference between the curves obtained in the known and unknown cases.

According to [5], it was concluded that when the uncertainty of the shape parameter is $1.5 \leq C \leq 2$, it is better to assume *C=1.5* instead of the estimate, however, if $1 \leq C \leq 2$, it will be better to estimate the *C*. Figure 17 represents as a function of the *SCR* for different values of the false alarm probability.

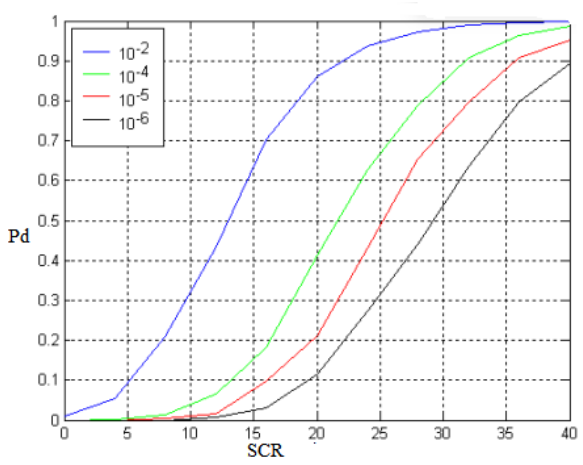

Figure 17: The probability of detection as a function of the *SCR*. Case of the OS-CFAR detector for *N=16* and *C=2*

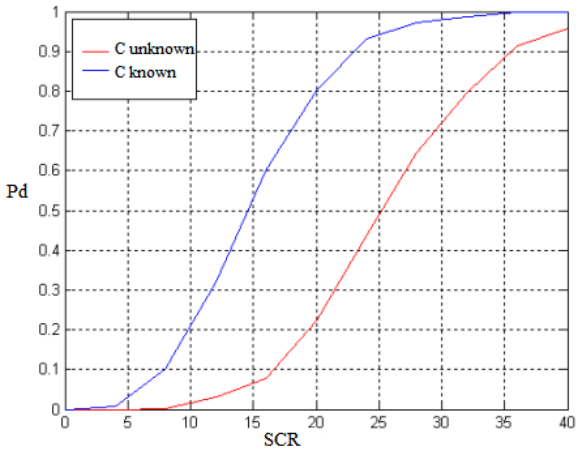

Figure 18: The probability of detection as a function of the *SCR*. Case of the OS-CFAR detector in the known and unknown case *C*. *N=16*, *Pfa=10-5* and *C=2*

Figure 18 represents a comparison of the detection probability variation as a function of the *SCR* when the shape parameter is known and unknown. The figure clearly shows the difference between the two cases. For an *SCR* equal to 0.5, the loss is equal to approximately *10dB* in the case where *i=3*, *j=16*, and *N=16* for a probability of false alarm equal to 10^{-5}.

We note that the loss of CFAR (CFAR loss) increases when the parameter *i* increases and the parameter *j* decrease. We can conclude that the estimated values of C cause a degradation of the probability of detection.

3.3. ML-CFAR detector

3.3.1. C shape parameter is known

The tables below represent the values of factor α for different values of *Pfa*, number *N*, and of the *C* shape parameter for the two cases where *C* is known and unknown:

Parameter	Cells	α		
C=1	N	Pfa=10^{-2}	Pfa=10^{-4}	Pfa=10^{-6}
	8	6.2262	17.2982	36.9873

	12	5.6136	13.8532	25.9473
	16	5.3363	12.4525	21.9420
	24	5.0767	11.2272	18.6787

Table 5: Values of α for different values of *Pfa* in the case of ML-CFAR (*C=1*)

Parameter	Cells	α		
C=2	N	Pfa=10^{-2}	Pfa=10^{-4}	Pfa=10^{-6}
	8	2.4952	4.1591	6.0817
	12	2.3693	3.7220	5.0939
	16	2.3101	3.5288	4.6842
	24	2.2531	3.3507	4.3219

Table 6: Values of α for different values of *Pfa* in the case of ML-CFAR (*C=2*)

Parameter	Cells	α		
C=3	N	Pfa=10^{-2}	Pfa=10^{-4}	Pfa=10^{-6}
	8	1.8397	2.5862	3.3318
	12	1.7772	2.4017	2.9605
	16	1.7475	2.3178	2.7996
	24	1.7187	2.2392	2.6533

Table 7: Values of α for different values of *Pfa* in the case of ML-CFAR (*C=3*)

In figures 19, 20, and 21, we plot the variations of the detection probability *Pd* as a function of the *SCR* for the ML-CFAR detector. These figures are obtained for a value of *Pfa* equal to 10^{-4}.

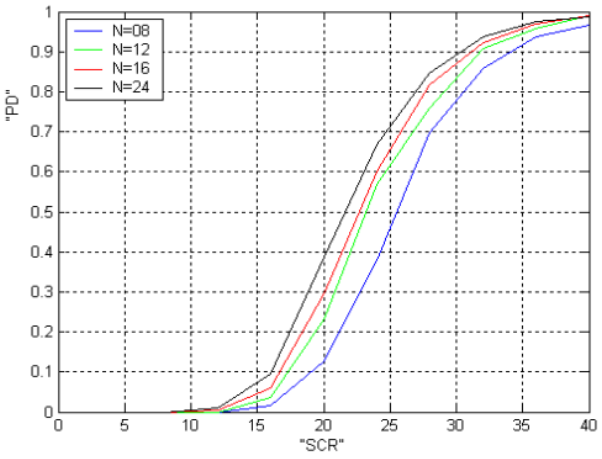

Figure 19: The probability of detection as a function of the *SCR*. Case of the ML-CFAR detector for *C=1* and *Pfa=10^{-4}*

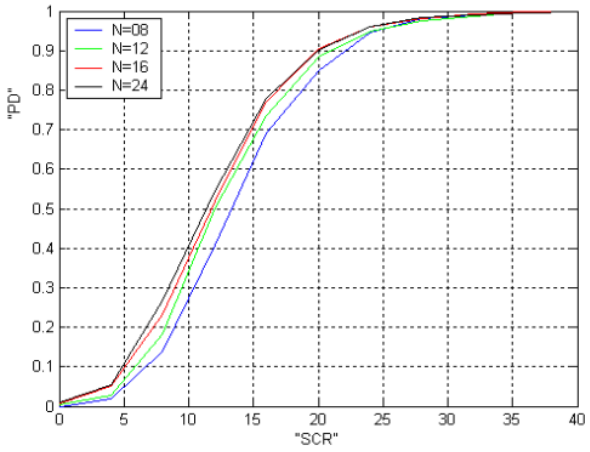

Figure 20: The probability of detection as a function of the *SCR*. Case of the ML-CFAR detector for *C=2* and $Pfa=10^{-4}$

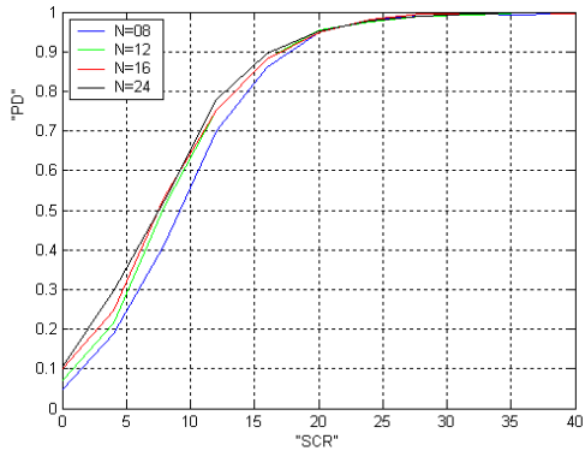

Figure 21: The probability of detection as a function of the *SCR*. Case of the ML-CFAR detector for *C=3* and $Pfa=10^{-4}$

In figure 22, we present the variation of the detection probability *Pd* as a function of the *SCR* for a *Pfa* equal to 10^{-5} and several cells equal to 16 for different values of the *C* shape parameter.

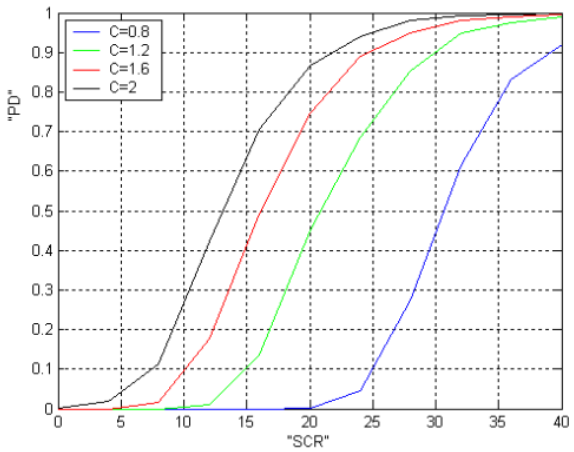

Figure 22: The probability of detection as a function of the *SCR*. Case of the ML-CFAR detector for *N=16* and $Pfa=10^{-5}$

We notice that in the case *C=0.8*, *1.2*, and *1.6*, the Pd remains zero for positive values of the *SCR* up to a value of the *SCR* equal to *20*, *8.5*, and *4 dB*, respectively, which means that the system is not reliable, because it ignores the information

for great values of the *SCR*. In the case where *C=2*, the graph starts at the origin and increases with the increase of the *SCR*, which means that the system is more reliable than the other cases.

Figure 23 illustrates the variation of the probability of detection as a function of the *SCR* with a variation of the *Pfa* in the case where the *C* shape parameter equals *2*, and the number of cells equals *16*.

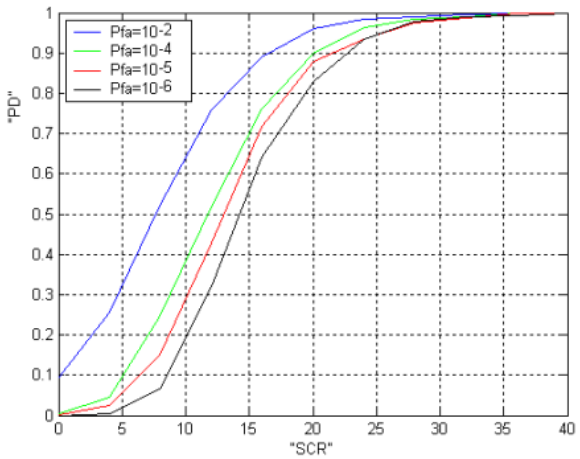

Figure 23: The probability of detection as a function of the *SCR*. Case of the ML-CFAR detector for *N=16* and *C=2*

For a *Pfa* equal to 10^{-6}, the probability remains zero for positive values of the *SCR* up to a precise value. On the other hand, for a *Pfa* equal to 10^{-2} and 10^{-4}, the *Pd* has a positive value of around 0.1 and 3.10^{-4}, respectively, for a zero *SCR*. It means that the system is not reliable since it ignores the information for great values of the *SCR*. In the case where *Pfa=10*$^{-5}$, the graph starts at the origin and increases with the increase of the *SCR*, which means that the system is more reliable compared to the other cases.

3.3.2. C shape parameter is unknown

When the scale parameter *B* and the shape parameter *C* are unknown, it is necessary to estimate them simultaneously.

In Figure 24, we present the variations of the probability of detection based on the *SCR* for an ML-CFAR detector; for different values of *C*, the parameters *B* and *C* are estimated using a maximum likelihood estimator.

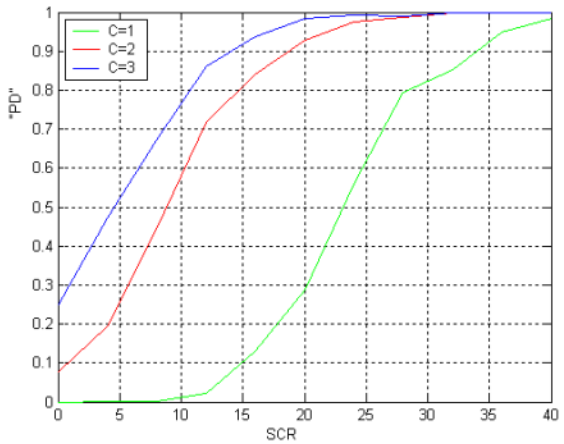

Figure 24: The probability of detection as a function of the *SCR*. Case of the ML-CFAR detector for *N=16* and *Pfa=10*$^{-4}$

Figure 25 illustrates the variation of the probability of detection as a function of the *SCR* and the probability of false alarm *Pfa*.

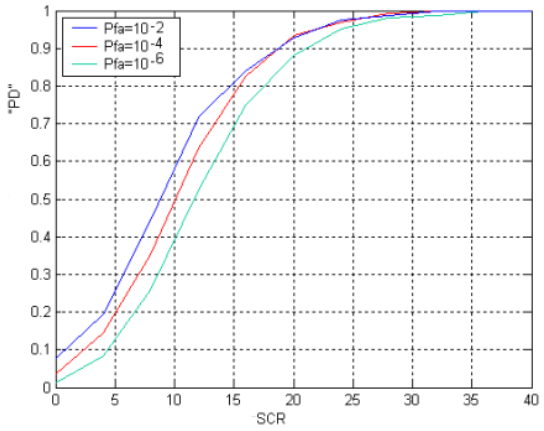

Figure 25: The probability of detection as a function of the *SCR*. Case of the ML-CFAR detector for *N=16* and *C=2*

Figure 26 presents a comparison between the case of known *C* and the case of unknown *C*. It is remarkable from this figure and figure 18 that the loss between the two curves is less than the loss obtained in the case of the OS-CFAR detector.

The simulation results indicate that the Maximum Likelihood estimator performs better than the Weber-Haykin estimator.

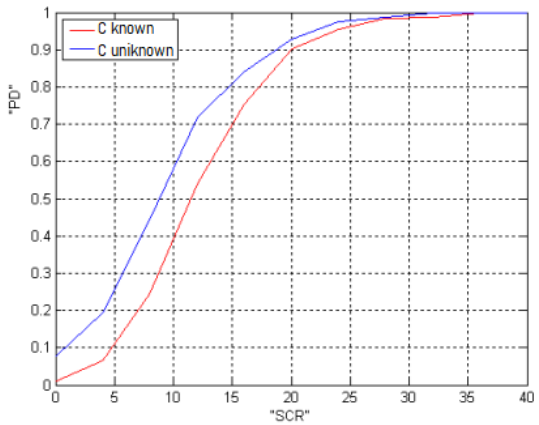

Figure 26: The probability of detection as a function of the *SCR*. Case of the ML-CFAR detector for *N=16*, *C=2*, and *Pfa=10*$^{-4}$

In this last part, we have presented all the results obtained using the Monte Carlo simulation. We have studied the OS-CFAR and ML-CFAR detectors in an environment which presents a homogeneous clutter by using the approach which considers the radar echoes which come from independent and identical reflections.

The model used is the Weibull model, this model is suitable for modeling sea clutter in which the shape parameter *C* proposes to be known or sometimes unknown.

Several methods can be used to estimate the value of *C*. For ML-CFAR, the Maximum-likelihood estimator showed a performance improvement compared to the Weber-Haykin estimator. The main characteristic of the maximum likelihood estimator is that it uses all these cells; for that, the algorithm presents a lower CFAR loss, and the deviation between the actual values and the estimated values are smaller. On the other hand, all the detectors show a better performance for a *Pfa* equal to 10^{-5} and a C shape parameter equal to 2, representing the Rayleigh distribution.

Conclusion

This work proposes to study and deal with the problem of CFAR detection in a sea clutter represented by a Weibull distribution. For this, we have chosen to use two types of detectors, the OS and the ML-CFAR, to determine their performance in different situations. These situations are presented according to the variation in the number of cells, the variation of the Pfa, and the variation of the shape parameter *C*. A comparison was carried out for several parameters by simulation according to the Monte Carlo method to determine the best between different types of detectors.

This study allowed us, in the first place, to note that the Weibull distribution model, which is the most suitable for the representation of sea clutter, is generally compared to other models because each change made in the shape parameter *C* represents another model. Also, the shape parameter C can present two different situations depending on whether *C* is known or unknown. In the second case, this parameter can be estimated using several methods. For ML-CFAR, the Maximum-likelihood estimator showed improved performance compared to the Weber-Haykin estimator. The main characteristic of the Maximum-likelihood estimator is that it uses all these cells; for that, the algorithm presents a lower CFAR loss, and the deviation between the real values and the estimated values are smaller.

In general, although it has been found that the best detector is the ML-CFAR, all the detectors present a better performance for a *Pfa* equal to 10^{-5} and a shape parameter *C* equal to 2, representing the Rayleigh distribution.

References :

[1] A.Hadjlarbi et Bellache Eliasse, « Etude comparative des Détecteurs CFAR et les systèmes distribuées en présences de cibles interférentes », Mémoire d'ingénieur, Département d'électronique, université de M'sila, 2004.

[2] Mourad baracat, "Signal detection and estimation" Artech and house 2005.

[3] M. Barkat. « Signal detection and estimation », Artech house radar library, MA 02062, 2iémé édition 2006.

[4] B. Atrouz, « Les systèmes radar », Ecole militaire polytechnique.

[5] N. Levanon, and M. Shor, « Order statistics CFAR for Weibull background, » IEE Proc., Vol. 137, Pt. F, (3), pp.157-162, June 1990.

[6] Y. Dong, « Distribution of X-Band High Resolution and High Grazing Angle Sea Clutter, » Commonwealth d'Australie 2006, AR-013-708, July 2006.

[7] R. Ravid, and N. Levanon, « Maximum likelihood CFAR for Weibull background, » IEE Proc. F., vol 139, N° 3, pp.256-264, June 1992.